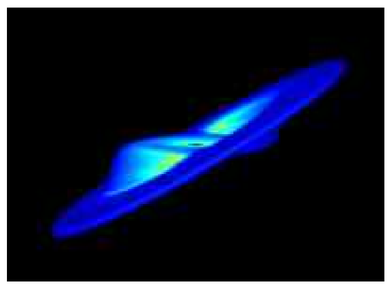

Constraining black hole spins through relativistic precession of accretion discs

Alessia Franchini[1], **Giuseppe Lodato**[1] **and Sara Elisa Motta**[2]

1. Dipartimento di Fisica, Università Degli Studi di Milano, Via Celoria, 16, Milano, I-20133, Italy

2. University of Oxford, Department of Physics, Astrophysics, Denis Wilkinson Building, Keble Road, OX1 3RH, Oxford , UK

Correspondence: alessia.franchini@unimi.it

Introduction

In this contribution we discuss the possibility to observe the **Lense-Thirring precession** of accretion discs around Kerr black holes in two type of systems: a newly formed accretion disc after the tidal disruption of a star by a supermassive black hole (TDE) and the inner accretion flow in a black hole low mass X-ray binary (LMXB). In both context the Lense-Thirring precession allows to place constraints on the black hole spin value.

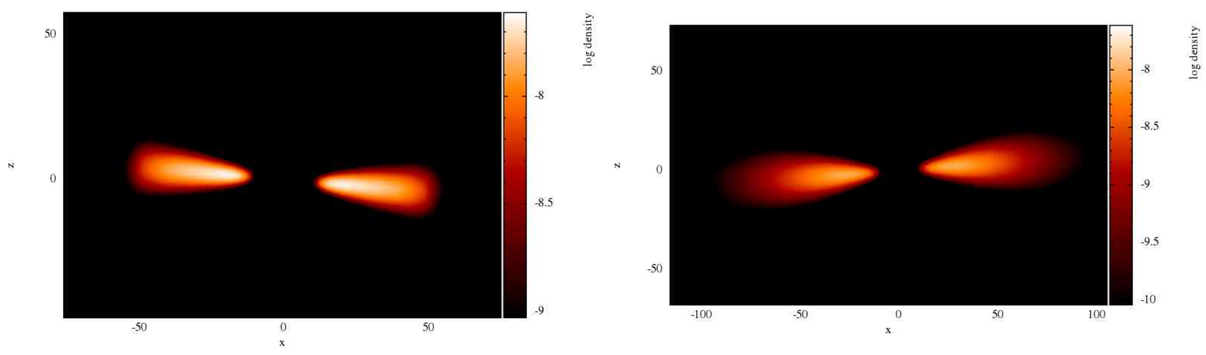

Figure 1: Surface density profile of a tilted accretion disc around a Kerr black hole obtained using the SPH code PHANTOM (Price et al., 2017)

Fig. 1 shows two snapshots of the disc surface density in the $x-z$ plane of an accretion disc inclined by 5 degrees with respect to the black hole spin. The left panel is the initial configuration while the right panel shows the disc after half a precession round. The rigid precession period is in perfect agreement with both the theoretical and ring code results.

Tidal Disruption Event discs

The debris of a tidally disrupted star are expected to form a thick and narrow accretion disc around the supermassive black hole. Since the initial star orbit is in general inclined with respect to the black hole plane, the disc angular momentum ends up being misaligned with the black hole spin. This misalignment leads to a warp in the disc due to the Lense-Thirring effect. A warped disc can precess as a rigid body around the black hole. The light curves of these events sometimes show a quasi-periodic modulation of the flux. We wondered if it could be the disc rigid precession causing the jet precession and thus the quasi-periodic behaviour in the light curve (Stone & Loeb, 2012; Lei et al., 2013; Shen & Matzner, 2014). We developed a model in order to evaluate the precession period and compare it with observations with the final purpose to provide a link between this observable and the supermassive black hole spin value.

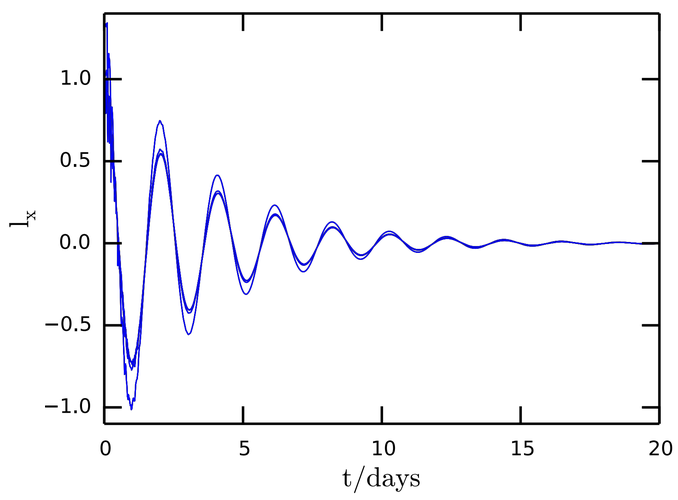

Figure 2: Evolution of the x-component of the disc angular momentum vector as a function of time. Black hole parameters: mass $M = 10^6 M_\odot$ and spin $a = 0.9$.

Fig. 2 shows the precession of the disc angular momentum vector as a function of time. It has been obtained solving the linearized wave equations for the warp propagation inside the disc with a ring code.

Results

The disc local precession frequency due to the Lense-Thirring effect is $\Omega_{\rm LT}(R) \propto R^{-3}$. The disc global precession frequency is the ratio between the total torque exerted on the disc and the disc angular momentum:

$$\Omega_{\rm p} = \frac{\int_{R_{\rm in}}^{R_{\rm out}} \Omega_{\rm LT}(R) L(R) 2\pi R\, dR}{\int_{R_{\rm in}}^{R_{\rm out}} L(R) 2\pi R\, dR}.$$

The resulting global precession period $t_{\rm p} = 2\pi/\Omega{\rm p}$ is shown in the left panel of Fig. 3 for both prograde and retrograde orbits.

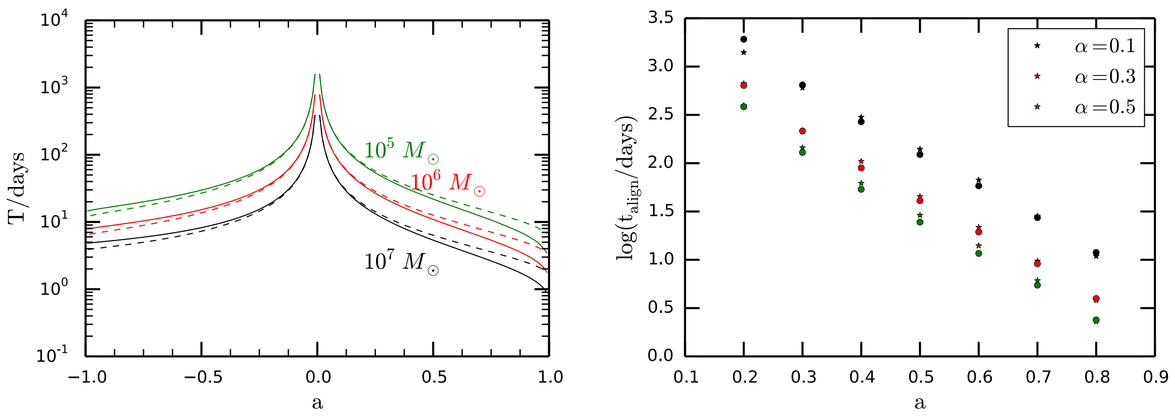

Figure 3: Left panel: global precession period as a function of the spin a (prograde and retrograde orbits) for different black hole mass ranging in $M = 10^5 - 10^7 M_\odot$. The dashed line represent the evolution with first order approximation in the expression for the local precession frequency. Right panel: alignment timescale as a function of the black hole spin for different values of the viscosity parameter α. The stars refer to values obtained with the ring code while the dots are obtained computing the alignment timescale given in Foucart & Lai (2014).

The higher the black hole spin, the closer is the disc inner radius to the black hole. The torque that warps the disc is thus stronger and results in a faster global precession of the disc. Prograde discs are expected to have shorter precession periods (of the order of $1 - 10$ d), while retrograde discs are characterized by much longer periods that would be harder to detect.

In Fig. 2 we can see that the periodicity of the x-component of the disc angular momentum drops after roughly a month. After some precession periods, when the warp is completely dissipated, the disc angular momentum ends up aligned with the black hole spin. The mechanisms that are likely to lead to alignment are either the decrease of the disc thickness, as a consequence of the decrease of the accretion rate with time, that causes the warp propagation to occur in the diffusive regime in which rigid precession cannot occur (Stone & Loeb, 2012) or the natural disc viscosity that damps the precession at a rate which is inversely proportional to the viscosity parameter value ($t_{\rm align} \propto \alpha^{-1}$). We found that for spin $a > 0.3$ the alignment is likely to be driven by the presence of the natural disc viscosity. We evaluate the timescale calculated by Foucart & Lai (2014) and compare them with our ring code simulations. The right panel of Fig. 3 shows that there is very good agreement.

It is worth noticing that there is degeneracy in mass and spin for each rigid precession period. **Measuring both the rigid precession period and the alignment timescale from the light curve of the event allows to break the degeneracy in mass and spin values**.

For details see Franchini et al. (2016).

Low Mass X-ray Binaries

The Lense-Thirring effect can be also used to place constraints on the black hole spin in the case of an X-ray binary through the detection of type-C Quasi-Periodic Oscillations (QPOs) in the power density spectra of these sources. According to the Relativistic Precession Model (RPM) these features are caused by the rigid precession of the inner accretion flow around the black hole and the measurement of their frequencies allows to obtain suitable ranges of values for the spin of the black hole even if no independent mass measurement is available. Under the assumption that the outer thin accretion disc (orange in left panel of Fig. 4) in the HSS extends down or close to the innermost stable circular orbit (ISCO) and that type-C QPOs would arise at the inner edge of the accretion flow, we use the RPM to place constraints on the black hole spin assuming that the highest frequency type-C QPOs in the soft state we found are produced at $\sim r_{\rm ISCO}$.

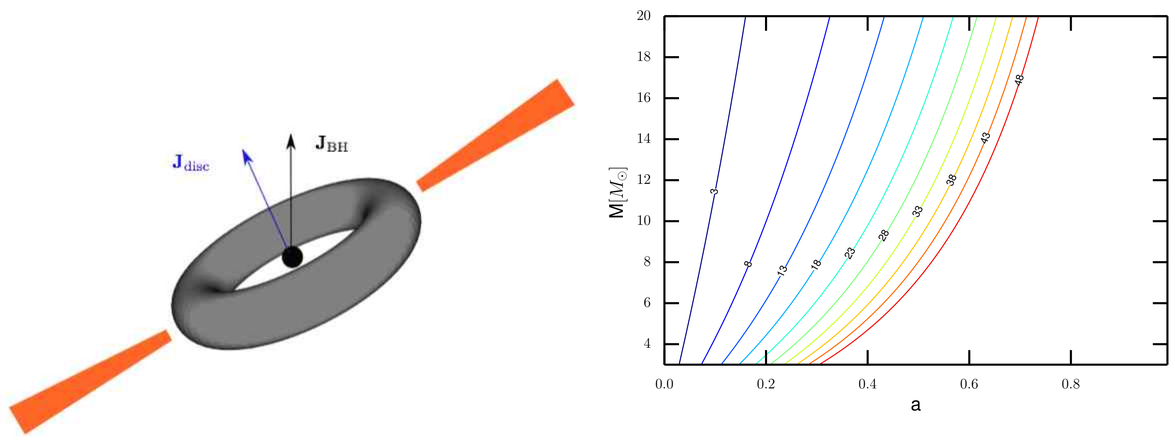

Figure 4: The left panel shows the inner accretion flow that precesses producing the type-C QPO. The right panel shows the couples of mass-spin values that give the LT precession frequency. The numbers are the frequencies evaluated in Hz.

Fig. 4 shows the Lense-Thirring precession frequency $\nu_{\rm LT}$ evaluated at $r_{\rm ISCO}$ for every mass and spin couple within the ranges $3M_\odot < M < 20M_\odot$ and $0 < a < 1$ (i.e. we considered only prograde orbits).

Results

For each source of our sample we considered the highest frequency type-C QPO and then **we inferred the BH spin assuming a given mass range for the sources that did not have an independent mass estimate**. If the highest type-C QPO was not detected in the HSS we can only place a conservative lower limit.

Table 1: Spin limits inferred using the RPM, assuming a black hole mass in the range $3 - 20M_\odot$. In the case of GX339-4 the lower limit corresponds to $6M_\odot$. For XTE J1550-564 and GRO J1655-40 the limits correspond to the measured masses $9.1 \pm 0.6 M_\odot$ and $5.31 \pm 0.07 M_\odot$ respectively (Muñoz Darias et al., 2010; Motta et al., 2014a,b). The first column contains the name of the source, the second is the highest type-C QPO frequency, the third column indicates the state in which the QPO was detected and the last column contains the spin limits.

Target	$\nu_{\rm max}$ (Hz)	state	spin limits
GX 339-4	10.59 ± 0.18	HSS	0.16 - 0.38
4U 1630-47	14.80 ± 0.28	ULS	> 0.12
4U 1543-47	15.37 ± 0.18	HSS	0.13 - 0.47
XTE J1859+226	8.56 ± 0.06	HIMS	> 0.07
XTE J1650-500	6.84 ± 0.05	HIMS	> 0.06
XTE J1817-330	9.6 ± 0.5	HSS	0.08 - 0.36
XTE J1748-288	31.55 ± 0.13	HIMS	> 0.23
XTE J1752-223	6.46 ± 0.13	HIMS	> 0.06
XTE J1550-564	18.10 ± 0.06	HSS	0.31 - 0.34
MAXI J1543-564	5.72 ± 0.04	HIMS	> 0.05
H1743-322	14.6 ± 0.2	ULS	> 0.12
GRO J1655-40	27.51 ± 0.13	HSS	0.29 - 0.31

We found type-C QPOs in the HSS for several sources of our sample. Applying the RPM to the highest frequency type-C QPO we were able to either place lower limits or to give a range for the black hole spin. We also compared the results obtained with spectroscopic measurements and we found good agreement for the two sources 4U 1543-47 and XTE J1550-564.

For details see Franchini et al. (2017).

References

Foucart F., Lai D., 2014, MNRAS, 445, 1731

Franchini A., Lodato G., Facchini S., 2016, MNRAS, 455, 1946

Franchini A., Motta S. E., Lodato G., 2017, MNRAS, 467, 145

Lei W.-H., Zhang B., Gao H., 2013, ApJ, 762, 98

Motta S. E., Muñoz-Darias T., Sanna A., Fender R., Belloni T., Stella L., 2014a, MNRAS,

Motta S. E., Belloni T. M., Stella L., Muñoz-Darias T., Fender R., 2014b, MNRAS, 437, 2554

Muñoz Darias T., Stiele H., Belloni T., Motta S., 2010, The Astronomer's Telegram, 2999, 1

Price D. J., et al., 2017, preprint, (arXiv:1702.03930)

Shen R.-F., Matzner C. D., 2014, ApJ, 784, 87

Stone N., Loeb A., 2012, Physical Review Letters, 108, 061302